

1 **Authors:** Jeremy D Wong, Tyler Cluff, Arthur D Kuo
2 **Affiliation:** University of Calgary, Faculty of Kinesiology, Department of Biomedical Engineering
3 **Corresponding author address:** Jeremy.wong2@ucalgary.ca
4 **Title:** The energetic basis for smooth human arm movements
5 **Running title:** Energetic basis for smooth human arm movements
6 **Key words:** metabolic energetic cost, reaching, minimum variance, minimum jerk, calcium
7 transport, muscle activation cost

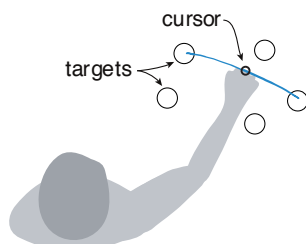
8 Abstract

9 The central nervous system plans human reaching movements with stereotypically smooth
10 kinematic trajectories and fairly consistent durations. Smoothness seems to be explained by
11 accuracy as a primary movement objective, whereas duration seems to avoid excess energy
12 expenditure. But energy does not explain smoothness, so that two aspects of the same
13 movement are governed by seemingly incompatible objectives. Here we show that smoothness
14 is actually economical, because humans expend more metabolic energy for jerkier motions. The
15 proposed mechanism is an underappreciated cost proportional to the rate of muscle force
16 production, for calcium transport to activate muscle. We experimentally tested that energy cost
17 in humans (N=10) performing bimanual reaches cyclically. The empirical cost was then
18 demonstrated to predict smooth, discrete reaches, previously attributed to accuracy alone. A
19 mechanistic, physiologically measurable, energy cost may therefore unify smoothness and
20 duration, and help resolve motor redundancy in reaching movements.

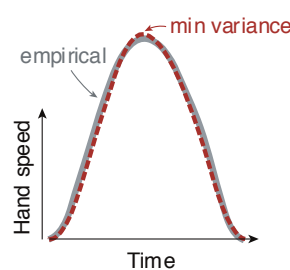
21

22 Introduction

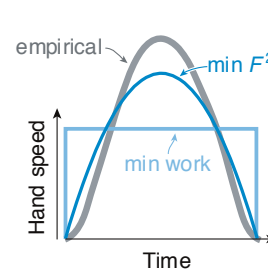
A. Reaching tasks



B. Performance objectives



C. Effort objectives



23

24 Figure 1. Goal-directed reaching tasks and optimization criteria. (A.) Typical experiments for point-to-point
25 movements between targets. (B.) Hand speed trajectories vs. time. Kinematic objectives such as minimizing jerk or
26 variance predict the observed smooth, bell-shaped profiles for hand speed. (C.) Effort-based objectives such as
27 minimizing work or squared muscle force or activation predict trajectories that are not smooth, or not bell-shaped
28 (Nelson 1983).

29

30

31 Upper extremity reaching movements are characterized by a stereotypical, bell-shaped speed
32 profile for the hand's motion to its target (Fig. 1A). The profile's smoothness seems to preserve
33 kinematic accuracy (Harris and Wolpert 1998), and have little to do with the effort needed to
34 produce the motion. But effort or energy expenditure appear to affect other aspects of

35 reaching (Huang et al. 2012; Shadmehr et al. 2019), and influence a vast array of other animal
36 behaviors and actions (Alexander 1996). It seems possible that effort or energy do influence the
37 bell-shaped profile, but have gone unrecognized because of incomplete quantification of such
38 costs. If so, then dynamic goals including effort could play a key role in movement planning.

39

40 The kinematic goal for accuracy may be expressed quantitatively as minimization of the final
41 endpoint position variance (Harris and Wolpert 1998). Non-smooth motions introduce
42 inaccuracy because motor noise increases with motor command amplitude, a phenomenon
43 termed signal-dependent noise (Matthews 1996; Sutton and Sykes 1967). It predicts well the
44 speed profiles for not only the hand but also the eye. It explains why more curved or more
45 accurate motions need to be slower, and also subsumes an older theory for minimizing
46 kinematic jerk (Flash and Hogan 1985). The single objective of movement variance explains
47 multiple aspects of smooth movements, and makes better predictions than competing theories
48 (Diedrichsen et al. 2010; Haith et al. 2012; Todorov 2004).

49

50 There are nonetheless reasons to consider effort. Many optimal control tasks must include an
51 explicit objective for effort, without which movements would be expected to occur at maximal
52 effort (“bang-bang control,” Harris and Wolpert 1998; Bryson and Ho 1975). In addition,
53 metabolic energy expenditure is substantial during novel reaching tasks, and decreases as
54 adaptation progresses (Huang et al. 2012). Such a cost also helps to determine movement
55 duration and vigor (Shadmehr et al. 2016), not addressed by the minimum-variance hypothesis.
56 Indeed, optimal control studies have long examined effort costs such as for muscle force
57 (Kolossatis et al. 2016), mechanical work (Alexander 1997), squared force or activation (Nelson
58 1983; Ma et al. 1994), or “torque-change” (integral of squared joint torque derivatives; Uno et
59 al. 1989). But such costs produce non-smooth velocity profiles (Fig. 1B), or lack physiological
60 justification, or both. Some studies have included explicit models of muscle energy expenditure,
61 but without testing such costs physiologically (Kistemaker et al. 2010). There is good evidence
62 that energy expenditure is relevant to reaching (Shadmehr et al. 2016), but no physiologically
63 tested cost function predicts the velocity profiles of reaching as well as the minimum variance
64 hypothesis.

65

66 The issue could be that metabolic energy expenditure for muscle is not quantitatively well-
67 understood. Energy is expended in proportion to force and time (“tension-time integral”) in
68 isometric conditions (Crow and Kushmerick 1982), and in proportion to mechanical work in
69 steady work conditions (Barclay 2015; Margaria 1976), neither of which apply well to reaching.
70 There is, however, a less-appreciated cost for muscles that increases with brief bursts of
71 intermittent or cyclic action. It is due to active calcium transport to activate/deactivate muscle,
72 observed in both isolated muscle preparations (Hogan et al. 1998) and whole organisms
73 (Bergstrom and Hultman 1988). It has also been hypothesized quantitatively (Doke and Kuo
74 2007), as a cost per contraction roughly proportional to the rate of change of muscle force.
75 Such a cost has indeed been observed in a variety of lower extremity tasks (Dean and Kuo 2011;
76 Doke et al. 2005; van der Zee and Kuo 2020). It has a mechanistic and physiological basis, is
77 supported by experimental evidence, and would appear to penalize jerky motions due to their
78 energetic cost. What is not known is whether this energetic cost can explain reaching.

79

80 We therefore tested whether there is an energetic basis for reaching movements. We did so by
81 measuring oxygen consumption during steady-state cyclic reaching motions. The expectation
82 was that the proposed force-rate cost would cost metabolic energy in excess of what could be
83 explained by mechanical work. We next applied the empirically derived cost for both force-rate
84 and work to an optimal control model of discrete, point-to-point reaching, and tested whether
85 it could predict the smooth, bell-shaped velocities normally attributed to minimum-variance. If
86 the proposed cost is observed as expected and predicts bell-shaped profiles, it could potentially
87 provide a re-interpretation of existing theories based on kinematics alone, and integrate energy
88 expenditure into a general framework for planning reaching movements.

89

90 Materials and Methods

91 There were three main components to
92 this study: (1) a simple cost model, (2) a
93 set of human subjects experiments with
94 cyclic reaching, and (3) an application of
95 the model to predict discrete reaching
96 trajectories. The model predicts that
97 metabolic cost should increase with the
98 hypothesized force-rate measure,
99 particularly for faster frequencies of
100 movement. Key to the experiment (Fig.
101 2) was to isolate the hypothesized force-
102 rate cost, by applying combinations of
103 movement amplitude and frequency that
104 control for the cost of mechanical work.
105 This primary test was accompanied by a
106 secondary, cross-validation test, with
107 different combinations of movement
108 amplitude and frequency. Finally, we
109 applied this same force-rate cost to the
110 prediction of discrete reaching
111 movement trajectories. This was to test whether the energetic cost, derived from continuous,
112 cyclic reaching movements, could also predict the smooth, discrete motions often found in the
113 literature.

114

115 Model predictions for force-rate hypothesis

116 We hypothesized that the energetic cost for reaching includes a cost for performing mechanical
117 work, and another for the rate of force production. These costs are implemented on a simple,
118 two-segment model of arm dynamics, actuated with joint torques. These torques perform work
119 on the arm, at an approximately proportional energetic cost (Margaria 1976) attributed to
120 actin-myosin cross-bridge action (Barclay 2015). The force-rate cost is hypothesized to result
121 from rapid activation and deactivation of muscle, increasing with the amount of force and

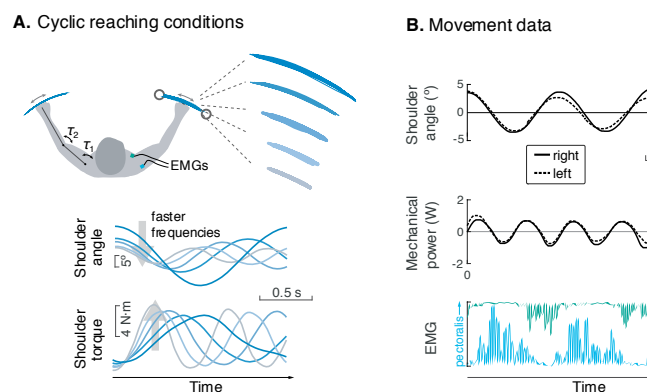


Figure 2. Experiment for metabolic cost of cyclic reaching. (A) Cyclic reaching was performed bimanually and symmetrically in the horizontal plane, primarily about the shoulders. To isolate the hypothesized force-rate cost from the energetic cost of work, movements were varied to yield fixed mechanical power, by decreasing amplitudes with increasing movement frequency. (B) Movement data included shoulder angle, mechanical power, electromyography (EMG), and (not shown) metabolic energy expenditure via expired gas respirometry.

122 inversely with the time duration. It is attributable to active transport of myoplasmic calcium
123 (Bergstrom and Hultman 1988; Hogan et al. 1998), where more calcium is required for higher
124 forces and/or shorter time durations, hence force-rate (Doke and Kuo 2007).

125

126 For the simple motion employed here, the prediction of the total energy E consumed per
127 movement is the sum of costs for work and force-rate,

$$E = c_W W + E_{FR} \quad (1)$$

128 where W is the positive mechanical work per movement, c_W the energetic cost for work, and
129 E_{FR} is the hypothesized force-rate cost

$$E_{FR} \propto \dot{F} \quad (2)$$

130

131 where \dot{F} denotes the amplitude of force-rate (time-derivative of muscle force) per movement.
132 (This cost is to be distinguished from the earlier torque-change hypothesis (Uno et al. 1989),
133 which integrates a sum-squared force-rate over time.) During cyclic reaching, the peak force-
134 rate \dot{F} increases with both force amplitude and the frequency of cyclic movement. Here,
135 positive and negative work are performed in equal magnitudes, and so their respective costs
136 are lumped together into a single proportionality c_W . We assigned c_W a value of 4.2, from
137 empirical mechanical work efficiencies of 25% for positive work and -120% for negative work
138 (Margaria et al. 1963).

139

140 The work and force of the cyclic reaching movements about the shoulder are predicted by a
141 simple model of arm dynamics. In the horizontal plane of a manipulandum supporting the arm,
142

$$T(t) = I \ddot{\theta}(t) \quad (3)$$

143

144 with shoulder angle $\theta(t)$, shoulder torque $T(t)$ (treated as proportional to muscle force), and
145 rotational inertia I . Applying sinusoidal motion at amplitude A and movement frequency f (in
146 cycle/s),

147

$$\theta(t) = A \cos 2\pi ft.$$

148

149 The torque is therefore

150

$$T(t) = -4\pi^2 I A f^2 \cos 2\pi ft$$

151

and amplitude of mechanical power \dot{W}

$$\dot{W} \propto A^2 f^3 \quad (4)$$

152

153 We apply a particular movement condition, termed the *fixed power* constraint (Fig. 2A), where
154 the average positive mechanical power is kept fixed across movement frequencies, so that the
155 hypothesized force-rate cost will dominate energetic cost (Fig. 3A). This is achieved by
156 constraining amplitude to decrease with movement frequency (Fig. 3B),

$$A \propto f^{-\frac{3}{2}} \quad (5)$$

157

158 This fixed power condition also means that hand (endpoint) speed, proportional to $\dot{\theta}$, should
159 have amplitude varying with $f^{-1/2}$, and torque amplitude with $f^{1/2}$ (Fig. 3C, D).

160

161 Applying fixed power to the force-rate cost yields a predicted energetic cost. Torque-rate
162 amplitude \dot{T} with Eqn. (5) and (2) yields

163

$$\dot{T} = b \cdot f^{\frac{3}{2}} \quad (6)$$

164

165 where b is a constant coefficient. The proportional cost per contraction is therefore (Eqn. (2))

$$E_{FR} = c_f \cdot f^{\frac{3}{2}} \quad (7)$$

166

167 where c_f is a constant coefficient across conditions. Experimentally, it is most practical to
168 measure metabolic power \dot{E} (Fig. 3a) in steady state. Multiplying E (cost per movement, Eqn.
169 (2) by f (movement cycles per time) yields the predicted proportionality for average metabolic
170 power,

$$\dot{E}_{FR} = c_f \cdot f^{5/2} . \quad (8)$$

171

172 The net metabolic rate \dot{E} is expected to increase similarly, but with an additional offset for the
173 constant work cost \dot{E}_W under the fixed-power constraint (Figure 3A). Finally, the metabolic
174 energy per time associated with force-rate would be expected to increase directly with torque-
175 rate per time $f \cdot \dot{T}$,

$$\dot{E}_{FR} = c_t \cdot f \cdot \dot{T} \quad (9)$$

176
177 where movement frequency f represents
178 cycles per time, and coefficient c_t is equal to
179 c_f divided by b .

181 Experiments

182 We measured the metabolic power expended
183 by healthy adults ($N = 10$) performing cyclic
184 movements at a range of speeds but fixed
185 power (Eqn. (5)). We tested whether
186 metabolic power would increase with the
187 hypothesized force-rate cost \dot{E}_{FR} , in amount
188 not explained by mechanical work. We also
189 characterized the mechanics of the task in
190 terms of kinematics, shoulder torque
191 amplitude, and force-rate for shoulder
192 muscles. These were used to test whether the
193 mechanics were consistent with the model of
194 arm dynamics, and whether force-rate
195 increased as predicted (Eqns. (5)-(8)). We first
196 describe a primary experiment with fixed
197 power conditions, followed by an additional
198 cross-validation experiment. All subjects
199 provided written informed consent, as
200 approved by University of Calgary Ethics
201 board.

202
203 Subjects performed cyclic bimanual reaching movements in the horizontal plane, with the arms
204 supported by a robotic exoskeleton (KINARM, BKIN Technologies, Inc). The exoskeleton was
205 used to counteract gravity in a low-friction environment (with no actuator loads), and to
206 measure kinematics, from which joint torques were estimated using inverse dynamics. Cyclic
207 movements were between two visual targets, reachable by medio-lateral shoulder motion
208 alone. There were however, no explicit constraints restricting free planar motions. The robot
209 displayed a 5mm visual cursor located at the hands and visual targets 2.5 cm diameter, all
210 optically projected onto the movement plane. A single visual cursor was displayed, as an
211 average of right and left arm joint angles, so that the task required visual tracking of only one
212 moving object. Timing was set with a metronome beat for each target, and amplitude by
213 adjusting the distance between the targets. Prior to data collection, subjects completed a 20-
214 minute familiarization session (up to 48 hours before the experiment) where they received task
215 instructions and briefly practiced each of the tasks.

216
217 The primary experiment was to test for the predicted energetic cost for reaching, in five
218 conditions of cyclic reaching at increasing frequency and decreasing amplitude. The frequencies

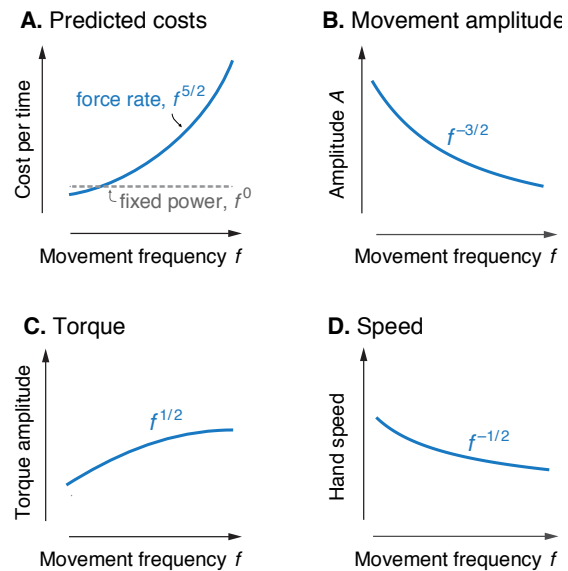


Figure 3. Predicted cost and dynamics for cyclic reaching, as a function of movement frequency f . (A.) Force-rate cost is predicted to increase with $f^{5/2}$, whereas cost for mechanical work is predicted to remain constant for fixed power conditions. (B.) Fixed power is achieved by specifying movement amplitude A to decrease with frequency, according to $f^{-3/2}$. (C.) Torque amplitudes are expected to increase modestly, with $f^{1/2}$. (D.) Peak hand speed is expected to decrease, with $f^{-1/2}$.

219 were 0.58, 0.78, 0.97, 1.17, 1.36 Hz, and amplitudes were 12.5, 8, 5.8, 4.4, 3.5°, respectively.
220 These cyclic movements were chosen to be of moderate hand speed, with peak speeds
221 between 0.4 – 0.6 m/s.

222
223 We estimated metabolic rate using expired gas respirometry. Subjects performed each
224 condition for 6 minutes, analyzing only the final 3 minutes of data for steady-state aerobic
225 conditions, with standard equations used to convert O₂ and CO₂ rates into metabolic power
226 (Brockway 1987). We report net metabolic rate \dot{E} , defined as gross rate minus the cost of quiet
227 sitting (obtained in a separate trial, 98.6 ± 11.5 W, mean \pm s.d.).

228
229 We also recorded arm segment positions and electromyographs simultaneously at 1000 Hz.
230 These included kinematics from the robot, and electromyographs (EMGs) from four muscles
231 (pectoralis lateral, posterior deltoid, biceps, triceps) in a subset of our subjects (5 subjects in
232 primary experiment, 5 in cross-validation). The EMGs were used to characterize muscle
233 activation and co-activation.

234
235 The metabolic cost hypothesis was tested using a linear mixed-effects model of net metabolic
236 power. This included the hypothesized force-rate cost (Eqn. 8) as a fixed effect, yielding
237 coefficient c_f for the force-rate term proportional to $f^{5/2}$. A constant offset was included for
238 each subject as a random effect. In addition, the force-rate cost \dot{E}_{FR} was estimated by
239 subtracting the fixed mechanical work cost \dot{E}_W from net metabolic power \dot{E} , and then
240 compared against torque rate amplitude per time (9).

241
242 We tested expectations for movement amplitude and other quantities from kinematic data.
243 Hand velocity was filtered using a bi-directional lowpass Butterworth filter (1st order, 12 Hz
244 cutoff). Shoulder torque was computed using inverse dynamics, based on KINARM dynamics
245 (BKIN Technologies, Kingston), and subject-specific inertial parameters (Winter 1990). The
246 approximate rotational inertia of a single human arm and exoskeleton about the shoulder was
247 estimated as 0.9 kg·m². The positive portion of mechanical power was integrated over total
248 movement duration and divided by cycle time, yielding average positive mechanical power.
249 Linear mixed-effects models were used to characterize the power-law relations for mechanical
250 power, movement amplitude, movement speed, torque amplitude, and torque rate amplitude
251 (Figure 3). The latter was estimated by integrating the torque rate amplitude per time (Eqn.
252 (9)). The force-rate hypothesis was also tested by comparing \dot{E}_{FR} with torque rate per time (Fig
253 3A), assuming torque is proportional to muscle force.

254
255 Electromyographs were used to test for changes in muscle activation and co-activation. Data
256 were mean-centred, low-pass filtered (bidirectional, second order, 30Hz cutoff), rectified, and
257 low-pass filtered again (Roberts and Gabaldón 2008), from which the EMG amplitude was
258 measured at peak and then normalized to each subject's maximum EMG across the five
259 conditions. We expected EMG amplitude to increase with muscle activation, with simplified
260 first-order dynamics between activation (EMG) and muscle force production (van der Zee and
261 Kuo 2020). This treats the rate-limiting step of force production as a low-pass filter, so that

262 greater activation or EMG amplitudes would be needed to produce a given force at higher
263 waveform frequencies. The first-order dynamics mean that EMG would be expected to increase
264 with torque rate $f^{3/2}$ rather than torque, as tested with a linear mixed-effects model. We also
265 computed a co-contraction index for EMG, in which the smallest value of antagonist muscle
266 pairs was computed over time, and then integrated for comparison across conditions (Gribble
267 et al. 2003). All statistical tests were performed with threshold for significance of $P < 0.05$.

268
269 We cross-validated the coefficient c_t by applying it to data collected in a second set of
270 conditions with a separate set of subjects (also $N = 10$; two subjects participated in both sets).
271 The conditions were slightly different: frequencies ranging 0.67 - 1.3 Hz and amplitudes 12.5 -
272 4.42°, which resulted in higher mechanical work and force-rate. The model (Eqns. (1), (9) applied
273 the c_t coefficient identified from the primary experiment to predict metabolic cost for the
274 cross-validation conditions, as a further test of the hypothesis.

275

276 Estimation of elastic energy storage in shoulder muscles

277 We estimated the resonant frequency of cyclic reaching, to account for possible series elasticity
278 in shoulder actuation. Series elasticity could potentially store and return energy and thus
279 require less mechanical work from muscle fascicles. We estimated this contribution from
280 resonant frequency, obtained by asking subjects to swing their arms back and forth rapidly at
281 large amplitudes (at least 15°) for 20 s, and determining the frequency of peak power (PWelch
282 in Matlab). We then used this to estimate torsional series elasticity, and the passive
283 contribution to mechanical power.

284

285 Musculoskeletal model to simulate experimental conditions

286 We tested whether a Hill-type musculoskeletal model could explain the metabolic cost of cyclic
287 reaching. The hypothesized force-rate is not explicitly included in current models of energy
288 expenditure, and would not be expected to explain the experimental metabolic cost. We
289 therefore tested an energetics model available in the OpenSim modeling system (Seth et al.
290 2018; Uchida et al. 2016; Umberger 2010), applied to a model of arm dynamics with six muscles
291 (Kistemaker et al. 2014). We used trajectory optimization to determine muscle states and
292 stimulations, with torques from inverse dynamics as a tracking reference. Optimization was
293 performed using TOMLAB and SNOPT (Gill et al. 2002), to minimize mean- square torque error,
294 squared stimulation level, and squared stimulation rate. The optimized muscle states were then
295 fed into the metabolic cost model (Umberger 2010).

296

297

298 Force-rate model to simulate energetic cost of point-to-point reaching

299 We hypothesized that force-rate minimization could predict smooth, bell-shaped velocity
300 profiles similar to minimum-variance. We tested this by performing trajectory optimization of
301 simulated planar, two-segment reaching movements, using the empirical force-rate coefficient
302 c_t (Eqns. (1), (9). Again, TOMLAB and SNOPT (Gill et al. 2002) were used to optimize shoulder
303 and elbow torques to minimize the hypothesized energy cost (Eqn. (1). The resulting hand
304 trajectory over time was then compared the minimum-variance model (Harris and Wolpert

305 1998). For minimum variance, we used 7 position-space knot points (linearly spaced in time)
 306 that minimized the variance of a straight reaching movement of amplitude 30 cm, movement
 307 duration 650 ms. Matching the model of Harris & Wolpert (1998), endpoint variance was
 308 averaged over a 500 ms hold period following movement end.

309

310 Results

311 The rate of metabolic energy expenditure increased substantially with movement frequency,
 312 even as the rate of mechanical work was nearly constant (Fig. 4A). Subjects expended more than
 313 triple (a factor of 3.56) the net metabolic power for about twice the frequency (a factor of 2.33),
 314 with 5.32 ± 2.73 W at the lowest frequency of 0.58 Hz, compared to 18.95 ± 6.02 W at the highest
 315 frequency of 1.36 Hz. As predicted, metabolic rate increased approximately with $f^{5/2}$ (Eqn. (7);
 316 adjusted $R^2 = 0.50$; $P = 1e-8$; Fig. 4a; Table 1).

317

Table 1. Experimental results. Linear mixed effects models were used to test model predictions from data. Listed for each quantity: predicted power law, estimated coefficient, 95% confidence interval (CI), R^2 , and P-value.

Quantity	Power law	Coefficient	95 % CI	R^2	P	Intercept
Metabolic Power \dot{E} (W)	$f^{5/2}$	6.72	(4.58, 8.86)	0.50	9.70E-9	3.93
Movement amplitude A (°)	$f^{3/2}$	5.97	(5.66, 6.28)	0.97	1.02E-39	-0.47
Peak speed amplitude (m·s ⁻¹)	$f^{-1/2}$	0.43	(0.39, 0.47)	0.93	6.63E-29	0.01
Torque amplitude (N·m)	$f^{1/2}$	8.34	(5.77, 10.91)	0.52	4.10E-9	1.63
Positive mechanical power \dot{W} (W)	f^0	1.20	(0.85, 1.55)			
Torque rate per time $f\dot{T}$ (N·m·s ⁻²)	$f^{5/2}$	78.93	(72.37, 85.48)	0.94	2.19E-30	46.43
EMG amplitude: Pec	$f^{3/2}$	0.17	(0.12, 0.23)	0.65	1.1E-6	0.17
EMG amplitude: Delt	$f^{3/2}$	0.20	(0.11, 0.27)	0.56	1.5e-5	0.20

318 Other aspects of the cyclic reaching task were as prescribed and intended (Fig. 4B-E; Table 1).
 319 Reach amplitudes decreased
 320 according to the targets,
 321 approximately with $f^{-3/2}$ (Fig.
 322 4B). Shoulder torque
 323 amplitude and endpoint speed
 324 also changed with respectively
 325 $f^{1/2}$ (Fig. 4C; adjusted $R^2 =$
 326 0.52 ; $P = 4e-9$) $f^{-1/2}$ (Fig. 4D;
 327 $R^2 = 0.93$; $P = 7e-29$).
 328 Consistent with the fixed-
 329 power condition, average
 330 positive mechanical power did
 331 not change significantly with
 332 frequency f (Fig. 4E; slope =
 333 $0.081 \pm 0.13 \text{ W}\cdot\text{s}^{-1}$; mixed-
 334 effects linear model with a
 335 fixed effect proportional to f^1 ,
 336 and individual subject offsets
 337 as random effects; $P = 0.16$).
 338 Amplitude of torque rate per
 339 time increased more sharply, approximately with $f^{5/2}$ (Fig. 4E), with coefficient b of $78.93 \pm$
 340 6.55 CI , 95% confidence interval).
 341

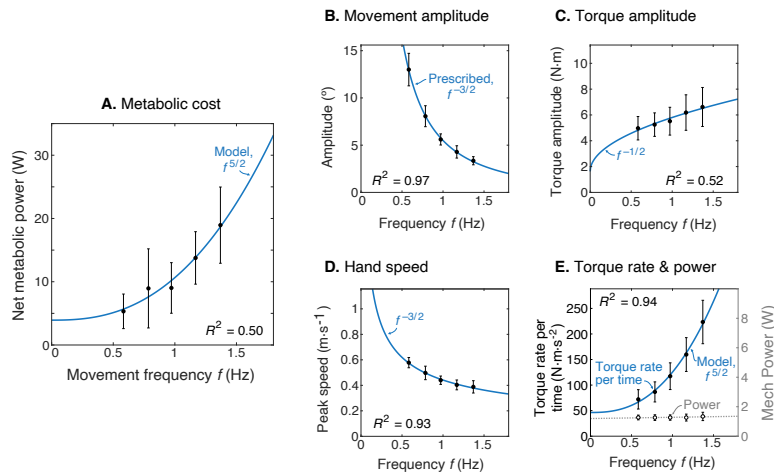


Fig 4. Experimental results as a function of movement frequency f . (A.) Net metabolic power \dot{E} vs. frequency f (means \pm s.d., $N = 10$), with predicted power law $f^{5/2}$ (solid line). (B.) Movement amplitude and prescribed target $f^{-3/2}$. (C.) Torque amplitude and prediction $f^{1/2}$. (D.) Hand speed amplitude and prediction $f^{-3/2}$. (E.) Amplitude of torque rate per time and prediction $f^{5/2}$, and mechanical power amplitude \dot{W} and constant power prediction.

342 The net metabolic cost was also consistent with the hypothesized sum of separate terms for
 343 positive mechanical work and force-
 344 rate (Fig. 5). This is demonstrated
 345 with metabolic power as a function
 346 of movement frequency f , and as a
 347 function of force-rate per time.
 348 With positive mechanical work at a
 349 fixed rate of about 1.2 W, the
 350 metabolic cost of work was
 351 expected to be constant at
 352 approximately 5 W. The difference
 353 between net metabolic rate and the
 354 constant work cost yielded the
 355 remaining force-rate metabolic
 356 power, increasing approximately
 357 with $f^{5/2}$ (Fig. 5A). This same force-
 358 rate cost could also be expressed as
 359 a linear function of the empirical
 360 torque rate per time, with an

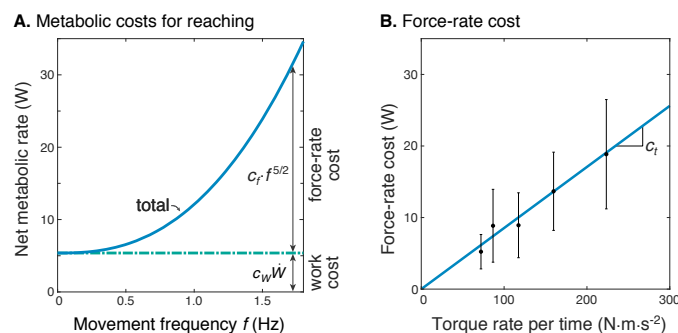


Fig. 5. Metabolic cost contributions from work and force-rate. (A.) Net metabolic rate \dot{E} vs. movement frequency f for cyclic reaching, with contributions from force-rate cost ($c_f f^{5/2}$) and mechanical work ($c_W \dot{W}$). Coefficient c_f was derived from experiment (Fig. 4), whereas c_W was specified as 4.2 to model a proportional cost for positive and negative mechanical work. (B.) Force-rate cost (metabolic power \dot{E}_{FR}) is linearly related to amplitude of torque rate per time $f\dot{T}$, by coefficient c_t determined from part A. and Fig. 4E.

361 estimated coefficient of $c_t=8.5e-2$ (Fig. 5B; see Eqn. (9). (Joint torque is treated as proportional
 362 to muscle force, assuming constant shoulder moment arm.) In terms of proportions,
 363 mechanical power accounted for about 94% of the net metabolic cost at 0.58 Hz, and 26% at
 364 1.36 Hz. Correspondingly, force-rate accounted for about 6% and 74% of net metabolic rate at
 365 the two respective frequencies.

366
 367 Muscle EMG amplitudes
 368 increased with movement
 369 frequency (Fig. 6). Deltoid and
 370 pectoralis both increased
 371 approximately with $f^{3/2}$
 372 (pectoralis: $R^2= 0.65$; $P = 1.1e-$
 373 6 ; deltoid: $R^2= 0.56$; $P = 1.5e-5$),
 374 as did the co-contraction index
 375 ($R^2= 0.58$; $P = 0.0009$). This
 376 was consistent with
 377 expectations of muscle
 378 activation increasing faster
 379 than torque for increasing
 380 movement frequencies.

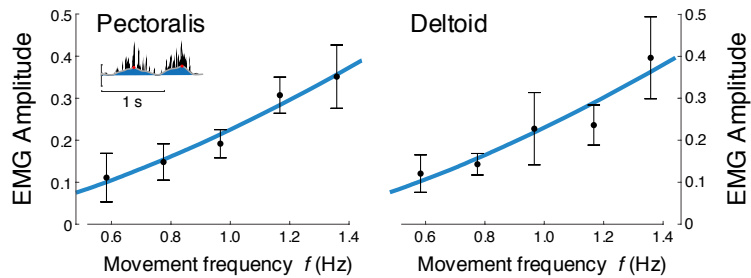


Fig. 6 EMG amplitude vs. movement frequency f during cyclic reaching. Inset figure depicts an example EMG rectified (black), filtered (blue), and amplitude (red). Pectoralis and deltoid EMGs (means \pm s.d.; $N = 10$), with best-fit predictions curves (both $f^{3/2}$), $R^2 = 0.65$ and $R^2 = 0.56$, respectively.

382 Cross-validation of metabolic cost during cyclic reaching

383 Separate cross-validation trials agreed well with force-rate coefficients. The second group of
 384 subjects moved with slightly
 385 increasing mechanical
 386 power, and slightly higher
 387 metabolic cost (Fig. 7). But
 388 applying the cost coefficient
 389 c_t derived from the primary
 390 experiment, the model
 391 (Eqns. 1 & 8) was
 392 nevertheless able to predict
 393 cross-validation costs
 394 reasonably well ($R^2 = 0.42$; P
 395 $= 2.7e-6$).

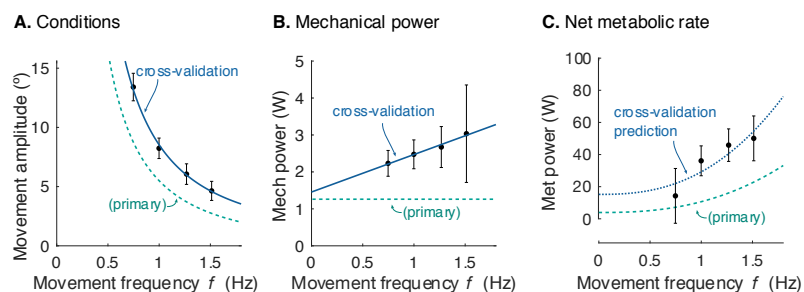


Fig 7. Cross-validation (CV) of force rate cost. (A.) Amplitude of cyclic reaching condition (compared with primary experiment) vs. movement frequency f and (B.) positive mechanical power \dot{W} vs. f . (C.) Net metabolic rate \dot{E} vs. movement frequency f for cross-validation (means \pm s.d.; $N = 10$). Cross-validation conditions were such that average positive mechanical power \dot{W} increased slightly with f , unlike the primary experiment. Predicted metabolic rate for CV was determined using c_t and c_W from primary experiment (solid line).

397 Passive elastic energy 398 storage during cyclic 399 reaching

400 The estimated natural frequency of cyclic arm motions was 2.83 ± 0.56 Hz. This suggests a
 401 rotational stiffness about the shoulder joint of about $250 \text{ N}\cdot\text{m}\cdot\text{rad}^{-1}$, if series elasticity were
 402 assumed for shoulder muscles. With passive elastic energy storage, the average positive
 403 mechanical power of muscle fascicles would decrease slightly, from about 0.5 W per arm to

404 0.33 W. Thus, series elasticity would cause active mechanical power to decrease with
405 movement frequency, as energy expenditure increased.

406

407 Hill-type model does not predict experimentally observed energy cost

408 The Hill-type model's predicted net energy cost increased approximately linearly with
409 movement frequency, from 33 W to 47 W. The model dramatically over-predicted the net
410 metabolic cost for all movements (by up to a factor of 6.2), and metabolic cost rose across
411 frequency by less than half as found experimentally (a factor of 1.42 vs. empirical 3.56). Current
412 musculoskeletal models do not accurately predict the cost of cyclic reaching.

413

414

415

416

417 Force-rate cost predicts point-to-point reaching

418 We applied the empirical force-rate coefficient c_t from
419 cyclic reaching (Fig. 5B) to predict discrete, point-to-point
420 reaching. We optimized the hypothesized energy cost (Eqn.
421 (1) for work and force-rate for a movement of fixed
422 duration (0.65 s) and distance (30 cm) comparable to that
423 reported previously (Harris and Wolpert 1998). The
424 optimization cost was implemented as an integral of
425 positive mechanical power and the absolute value of force-
426 rate per time, with respective coefficients c_W and c_t
427 derived from the primary experiment. The optimization
428 yielded bell-shaped velocities (Fig. 8) similar to the
429 minimum variance model and to empirical data (Harris and
430 Wolpert 1998).

431

432 Discussion

433 We tested whether the metabolic cost of reaching
434 movements is predicted by the hypothesized force-rate
435 cost. Our experimental data showed a cost increasing with
436 movement frequency as predicted with force-rate, more so
437 than did the mechanical work performed. The same cost model was also cross-validated with a
438 separate set of reaching movements, and predicts smooth reaching movements, similar to the
439 minimum variance model. We interpret these findings as suggesting the force-rate hypothesis
440 as an energetic basis for reaching movements.

441

442 The force-rate hypothesis explains the observed metabolic energy cost increases better than by
443 more conventionally recognized costs. For example, the cost of mechanical work cannot explain
444 the higher cost at higher movement frequencies, because the rate of work remained fixed (Fig.
445 5). A possible explanation is that the energetic cost per unit of work (c_W in Eqn. 1) could
446 increase with faster movements, due to the muscle force-velocity relationship (Barclay 2015).

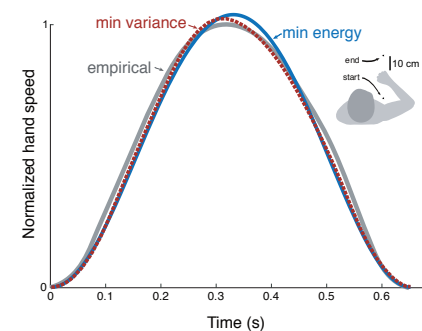


Fig 8. Hand speed trajectories for point-to-point movements predicted by energy expenditure and by minimum variance, with smooth, bell-shaped profiles. Minimum energy expenditure uses as its objective the summed costs of force-rate and work (Eqn. (1), with coefficient c_t specified from the primary experiment (Fig. 4). The minimum variance objective uses the covariance of movement error during a hold period at the target (Harris & Wolpert). Both optima use the same initial and final targets and a fixed movement duration.

447 But the conditions here actually yielded slower hand speeds with higher frequencies (Fig. 4D),
448 and thus cannot explain the higher cost. Nor were our results explained by a current
449 musculoskeletal model (Umberger 2010), which drastically overestimated the overall cost and
450 underestimated the increases with movement frequency. The proposed force-rate hypothesis
451 thus explains these data better than previous quantitative models or relationships.

452
453 The force-rate hypothesis was also consistent with three other observations: (1)
454 electromyography, (2) cross-validation, and (3) point-to-point reaching. First, muscle EMGs
455 increased more rapidly (approximately with $f^{3/2}$; Fig. 6) with movement frequency than did
456 joint torques (approximately with $f^{1/2}$; Fig. 4C). The proposed mechanism is that brief bursts of
457 activation require greater active calcium transport (and thus greater energy cost), because
458 muscle force production has slower dynamics than muscle activation (van der Zee and Kuo
459 2020). Second, we cross-validated the primary experiment, by applying its cost coefficients (c_t
460 and c_w , Fig. 5) to predict an independent set of conditions. We found good agreement between
461 cross-validation data and the force-rate prediction (Fig. 7). The overall energy cost (\dot{E} from Eqn.
462 1) depends on a particular combination of work, force, and movement frequency, yet only has
463 one degree of freedom (c_t). Third, the force-rate hypothesis also explains discrete, point-to-
464 point reaching. The characteristic bell-shaped velocity profile is predicted by optimal control,
465 using the cost coefficients derived from cyclic movements (Fig. 8). These observations serve as
466 falsifying tests of the force-rate hypothesis, independently predicted by a single model.

467
468 The force-rate cost is surely not the sole explanation for reaching. The optimal control approach
469 has been used to propose a variety of abstract mathematical objective functions that can
470 predict movement. But there may be multiple objectives that predict the same behavior. As
471 such, careful experimentation (Harris and Wolpert 1998; Kawato 1999) was required to
472 disambiguate minimum-variance from competing hypotheses such as minimum-jerk and -
473 torque-change (Kawato 1999). Similarly, the present study does not disambiguate force-rate
474 from minimum-variance, since both predict similar point-to-point movements. In fact,
475 minimum-variance also has some dependency on effort, albeit implicitly, due to the mechanism
476 of signal-dependent noise (Harris and Wolpert 1998). It also explains well the trade-off between
477 movement speed and endpoint accuracy, where energy expenditure is unlikely to be important.
478 However, the ambiguity also means that force-rate might alternatively explain aspects of
479 movements previously attributed to minimum-variance alone. Variance and explicit energy cost
480 could both potentially contribute to a unified objective for reaching.

481
482 Effort objectives have long been considered potential counterparts to the kinematic
483 performance objective. For example, the integrated squared muscle force or activation or
484 torque-change all emphasize effort and arm dynamics as explicit features for reaching (Uno et
485 al. 1989). Effort is also important for selection of feedback control gains (Kuo 1995; Todorov
486 and Jordan 2002), adaptation of coordination (Emken et al. 2007), identification of control
487 objectives from data (Vu et al. 2016) and determination of movement duration (Shadmehr et
488 al. 2016). In many such cases, effort was considered an abstract optimization variable, but was
489 not seriously considered to have a physiological and measurable representation as metabolic
490 energy expenditure. However, the adaptation of metabolic cost during adaptation (Huang et al.

491 2012) and the effect of metabolic state on reaching patterns (Taylor and Faisal 2018) strongly
492 suggest a role for energy in reaching. The present study offers a potential means to unify effort
493 in optimal control predictions with metabolic energy expenditure.

494

495 There is a measurable and non-trivial energetic cost for cyclic reaching. Even though the arms
496 were supported by a planar manipulandum, at a movement frequency of 1.5 Hz, we observed a
497 net metabolic rate of about 19 W. For comparison, the difference in cost between continuous
498 standing and sitting is about 24 W (Mansoubi et al. 2015), making the reaching task nearly as
499 costly as standing up. And per reaching movement, the metabolic cost (at two movements per
500 cycle) was about 7 J. This may be sufficiently high for the nervous system to prefer economical
501 ways to accomplish a reaching task.

502

503 There are several limitations to this study. One is that energetic cost was experimentally
504 measured for the whole body, and not distinguished at the level of the muscle. Force-rate was
505 also estimated from joint torque and not from actual muscle forces. We therefore cannot
506 eliminate other physiological processes as possible contributions to the observed energy cost.
507 In addition, the hypothesized cost (\dot{E}_{FR}) is thus far a highly simplified, conceptual model for a
508 muscle activation cost. More precise mechanistic predictions of this cost would be facilitated
509 with specific models for muscle activation, myoplasmic calcium transport, and force delivery
510 are needed (e.g., Baylor and Hollingworth 1998; Ma and Zahalak 1991). Additional experiments
511 could test the force-rate hypothesis further, and additional models could extend the
512 mechanistic basis for this cost.

513

514 The force-rate hypothesis suggests a substantial role for effort or energy expenditure in upper
515 extremity reaching movements. Some form of effort cost is often employed to examine
516 selection of feedback gains or muscle forces, and even generally expected for optimal control
517 problems where maximal-effort actions are to be avoided (Bryson and Ho 1975). And in the
518 experimental realm, energy expenditure is regarded as a major factor in animal life and
519 behavior (Alexander 1996), even to the small scale of a single neural action potential (Sterling
520 and Laughlin 2017). Under the minimum-variance hypothesis, reaching seems unusually
521 dominated by kinematics. But our results suggest that metabolic energy expenditure may have
522 been shadowed by the minimum-variance hypothesis, because it makes similar predictions for
523 point-to-point movements. There is need to both quantify and test the force-rate hypothesis
524 more specifically. Nonetheless, there is a meaningful energetic cost to reaching that can also
525 explain the smoothness of reaching motions.

526

527 [Acknowledgements](#)

528 This work was funded by NSERC (Discovery and CRC Tier 1), Dr. Benno Nigg Research Chair, and
529 Alberta Health Trust. We acknowledge Dinant Kistemaker for sharing simulation code for Hill-
530 type muscle model energetics.

531

532

533 [References](#)

534

535 **Alexander RM.** Optima for Animals [Online]. Princeton University
536 Press.<https://press.princeton.edu/books/paperback/9780691027982/optima-for-animals> [5
537 Sep. 2020].

538 **Alexander RMcN.** A minimum energy cost hypothesis for human arm trajectories. *Biol Cybern*
539 76: 97–105, 1997.

540 **Barclay CJ.** Energetics of contraction. *Compr Physiol* 5: 961–995, 2015.

541 **Baylor SM, Hollingworth S.** Model of sarcomeric Ca²⁺ movements, including ATP Ca²⁺ binding
542 and diffusion, during activation of frog skeletal muscle. *The Journal of general physiology* 112:
543 297–316, 1998.

544 **Bergstrom M, Hultman E.** Energy cost and fatigue during intermittent electrical stimulation of
545 human skeletal muscle. *Journal of Applied Physiology* 65: 1500–5, 1988.

546 **Brockway JM.** Derivation of formulae used to calculate energy expenditure in man. *Hum Nutr*
547 *Clin Nutr* 41: 463–471, 1987.

548 **Bryson AE, Ho Y-C.** *Applied Optimal Control*. New York: John Wiley & Sons, 1975.

549 **Crow MT, Kushmerick MJ.** Chemical energetics of slow- and fast-twitch muscles of the mouse. *J*
550 *Gen Physiol* 79: 147–166, 1982.

551 **Dean JC, Kuo AD.** Energetic costs of producing muscle work and force in a cyclical human
552 bouncing task. *J Appl Physiol* 110: 873–880, 2011.

553 **Diedrichsen J, Shadmehr R, Ivry RB.** The coordination of movement: optimal feedback control
554 and beyond. *Trends in Cognitive Sciences* 14: 31–39, 2010.

555 **Doke J, Donelan JM, Kuo AD.** Mechanics and energetics of swinging the human leg. *J Exp Biol*
556 208: 439–445, 2005.

557 **Doke J, Kuo AD.** Energetic cost of producing cyclic muscle force, rather than work, to swing the
558 human leg. *J Exp Biol* 210: 2390–2398, 2007.

559 **Emken JL, Benitez R, Sideris A, Bobrow JE, Reinkensmeyer DJ.** Motor adaptation as a greedy
560 optimization of error and effort. *Journal of neurophysiology* 97: 3997–4006, 2007.

561 **Flash T, Hogan N.** The coordination of arm movements: an experimentally confirmed
562 mathematical model. *J Neurosci* 5: 1688–1703, 1985.

563 **Gill P, Murray W, Saunders M.** Snopt - an SQP algorithm for nonlinear optimization. *Siam*
564 *Journal of Optimization* 12: 979–1006, 2002.

- 565 **Gribble PL, Mullin LI, Cothros N, Mattar A.** Role of cocontraction in arm movement accuracy. *J*
566 *Neurophysiol* 89: 2396–2405, 2003.
- 567 **Haith AM, Reppert TR, Shadmehr R.** Evidence for hyperbolic temporal discounting of reward in
568 control of movements. *J Neurosci* 32: 11727–11736, 2012.
- 569 **Harris CM, Wolpert DM.** Signal-dependent noise determines motor planning. *Nature* 394: 780–
570 784, 1998.
- 571 **Hogan MC, Ingham E, Kurdak SS.** Contraction duration affects metabolic energy cost and
572 fatigue in skeletal muscle. *Am J Physiol* 274: E397-402, 1998.
- 573 **Huang HJ, Kram R, Ahmed AA.** Reduction of metabolic cost during motor learning of arm
574 reaching dynamics. *J Neurosci* 32: 2182–2190, 2012.
- 575 **Kawato M.** Internal models for motor control and trajectory planning. *Current Opinion in*
576 *Neurobiology* 9: 718–727, 1999.
- 577 **Kistemaker DA, Wong JD, Gribble PL.** The Central Nervous System Does Not Minimize Energy
578 Cost in Arm Movements. *Journal of Neurophysiology* 104: 2985–2994, 2010.
- 579 **Kistemaker DA, Wong JD, Gribble PL.** The cost of moving optimally: kinematic path selection. *J*
580 *Neurophysiol* 112: 1815–1824, 2014.
- 581 **Kolossiatis M, Charalambous T, Burdet E.** How Variability and Effort Determine Coordination at
582 Large Forces. *PLoS One* 11, 2016.
- 583 **Kuo AD.** An optimal control model for analyzing human postural balance. *IEEE Trans Biomed*
584 *Eng* 42: 87–101, 1995.
- 585 **Ma B, Giat Y, Levine WS.** The Optimal Control of a Movement of the Human Upper Extremity1.
586 *IFAC Proceedings Volumes* 27: 455–460, 1994.
- 587 **Ma SP, Zahalak GI.** A distribution-moment model of energetics in skeletal muscle. *J Biomech* 24:
588 21–35, 1991.
- 589 **Mansoubi M, Pearson N, Clemes SA, Biddle SJ, Bodicoat DH, Tolfrey K, Edwardson CL, Yates T.**
590 Energy expenditure during common sitting and standing tasks: examining the 1.5 MET
591 definition of sedentary behaviour. *BMC Public Health* 15: 516, 2015.
- 592 **Margarita R.** *Biomechanics and energetics of muscular exercise.* Oxford, London, 1976.
- 593 **Margarita R, Cerretelli P, Aghemo P, Sassi G.** Energy cost of running. *J Appl Physiol* 18: 367–370,
594 1963.

- 595 **Matthews PB.** Relationship of firing intervals of human motor units to the trajectory of post-
596 spike after-hyperpolarization and synaptic noise. *The Journal of physiology* 492: 597–628, 1996.
- 597 **Nelson WL.** Physical principles for economies of skilled movements. *Biological cybernetics* 46:
598 135–147, 1983.
- 599 **Roberts TJ, Gabaldón AM.** Interpreting muscle function from EMG: lessons learned from direct
600 measurements of muscle force. *Integrative and comparative biology* 48: 312–320, 2008.
- 601 **Seth A, Hicks JL, Uchida TK, Habib A, Dembia CL, Dunne JJ, Ong CF, DeMers MS, Rajagopal A,**
602 **Millard M.** OpenSim: Simulating musculoskeletal dynamics and neuromuscular control to study
603 human and animal movement. *PLoS computational biology* 14: e1006223, 2018.
- 604 **Shadmehr R, Huang HJ, Ahmed AA.** A representation of effort in decision-making and motor
605 control. *Current biology* 26: 1929–1934, 2016.
- 606 **Shadmehr R, Reppert TR, Summerside EM, Yoon T, Ahmed AA.** Movement vigor as a reflection
607 of subjective economic utility. *Trends in Neurosciences* 42: 323–336, 2019.
- 608 **Sterling P, Laughlin S.** *Principles of Neural Design*. Reprint Edition. Cambridge: The MIT Press,
609 2017.
- 610 **Sutton GG, Sykes K.** The variation of hand tremor with force in healthy subjects. *The Journal of*
611 *Physiology* 191: 699–711, 1967.
- 612 **Taylor SV, Faisal AA.** Does internal metabolic state determine our motor coordination strategy?
613 *bioRxiv* 312454, 2018.
- 614 **Todorov E.** Optimality principles in sensorimotor control. *Nature neuroscience* 7: 907–915,
615 2004.
- 616 **Todorov E, Jordan MI.** Optimal feedback control as a theory of motor coordination. *Nat*
617 *Neurosci* 5: 1226–1235, 2002.
- 618 **Uchida TK, Hicks JL, Dembia CL, Delp SL.** Stretching your energetic budget: how tendon
619 compliance affects the metabolic cost of running. *PloS one* 11: e0150378, 2016.
- 620 **Umberger BR.** Stance and swing phase costs in human walking. *Journal of the Royal Society*
621 *Interface* 7: 1329–1340, 2010.
- 622 **Uno Y, Kawato M, Suzuki R.** Formation and control of optimal trajectory in human multijoint
623 arm movement. *Biological cybernetics* 61: 89–101, 1989.
- 624 **Vu VH, Isableu B, Berret B.** On the nature of motor planning variables during arm pointing
625 movement: Compositeness and speed dependence. *Neuroscience* 328: 127–146, 2016.

626 **Winter DA.** *Biomechanics and motor control of human movement*. New York, NY, US: John
627 Wiley & Sons, 1990.

628 **van der Zee TJ, Kuo AD.** The high energetic cost of rapid force development in cyclic muscle
629 contraction [Online]. *Journal of Experimental Biology* ,
630 2020<https://www.biorxiv.org/content/10.1101/2020.08.25.266965v1> [8 Sep. 2020].

631

632 .